PERFORMANCE OF META-MATERIAL THERMAL CONCENTRATOR WITH SENSU-SHAPED STRUCTURE THROUGH ENTROPY GENERATION APPROACH

by

Jiao-Long WANG[a], Hao-Chun ZHANG[a*], Chao MA[a], Cheng-Shuai SU[a], Han SHEN[b], and Gong-Nan XIE[b]

[a] School of Energy Science and Engineering, Harbin Institute of Technology, Harbin, China
[b] Department of Mechanical and Power Engineering, School of Marine Science and Technology, Northwestern Polytechnical University, Xi'an, China

Original scientific paper
DOI: 10.2298/TSCI16S3651W

A meta-material thermal concentrator model was simulated with different operating modes and different constructions based on sensu-shaped unit. The temperature and entropy generation rate was obtained by transient calculation. Thermal concentration ratio was defined with temperature and entropy production rate, which was used to analyze and evaluate performance. Thermal concentration ratio had the biggest value and thermal concentrator had the best effect at initial stage of the process. A larger temperature difference or smaller center distance leaded to better thermal control effect.

Key words: *meta-materials, thermal concentrator, numerical simulation, entropy generation, thermal concentration ratio*

Introduction

Unique performances of meta-material attract wide concerns, and it is significant to explore its performance. Veselago *et al.* [1] predicted left-handed materials through transformation of Maxwell equation. Schurig *et al.* [2] proposed a concept of transformation optics and electromagnetic meta-material cloak based on co-ordinate transformation and Maxwell equation transformation of practical material properties, and the concept was extended to many fields [3-6].

There were some challenges when optical meta-materials were applied to thermal field and the development of thermal meta-materials is relatively slow [7]. Fan *et al.* [8] designed a thermal meta-material to control the direction of the heat flux using transformation optics in heat diffuse equation. Brun *et al.* [9] achieved a circular thermal cloak, which extended transform theory to unsteady heat diffuse equation. Li *et al.* [10] realized the control of both current and heat flux, by changing thermal conductivity and electrical conductivity of materials. Guenneau *et al.* [11] designed a cylindrical thermal cloak and a thermal concentrator. Schittny *et al.* [12] created a circular layered material for protection and stealth of the central region, using a cyclic permutation of copper and polydimethylsiloxane (PDMS). Han *et al.* [13] produced a two-layer thermal cloak by utilizing PDMS and in conel 625 alloy. The structures of radial layer designed by Lan *et al.* [14] and sensu-shaped with PDMS and copper

* Corresponding author; e-mail: ces@vip.126.com

designed by Han *et al.* [15] can control both heat flow and current. Nguyen *et al.* [16] designed an active thermal cloaking device which can pump heat flux. Although several meta-materials with different microscale structures to control heat transfer were proposed, it is necessary to investigate the mechanism for energy transfer process and performance.

Since Gyftopoulos [17] introduced the concept of entropy, the second law approach has been applied to various fields. Entropy generation analysis plays a significant role on industrial production and becomes an evaluation indicator on the process of heat transfer and flow. In the current paper, a thermal concentrator structure unit with the circumferential arrangement of PDMS and copper was adopted based on a sensu-shaped unit [15], and the performance of was analyzed through entropy generation approach.

Mathematical and physical mode

For the heat conduction process in a 2-D Cartesian co-ordinates, entropy generation rate [18] of aninfinitesimal element dxdy can be expressed:

$$\dot{S}'''_{\mathrm{gen}}\mathrm{d}x\mathrm{d}y\mathrm{d}\tau = \rho c_{\mathrm{p}}\frac{1}{T}\frac{\partial T}{\partial \tau}\mathrm{d}x\mathrm{d}y\mathrm{d}\tau - \frac{q_x}{T}\mathrm{d}y\mathrm{d}\tau - \frac{q_y}{T}\mathrm{d}x\mathrm{d}\tau + \\ + \frac{q_x + \dfrac{\partial q_x}{\partial x}\mathrm{d}x}{T + \dfrac{\partial T}{\partial x}\mathrm{d}x}\mathrm{d}y\mathrm{d}\tau + \frac{q_y + \dfrac{\partial q_y}{\partial y}\mathrm{d}y}{T + \dfrac{\partial T}{\partial y}\mathrm{d}y}\mathrm{d}x\mathrm{d}\tau \tag{1}$$

where $\dot{S}'''_{\mathrm{gen}}$ is the entropy generation rate, τ – the time, T – the absolute temperature, q – the heat flux, c_p – the specific heat, and ρ – the density.

Dividing by xdydτ, entropy generation rate becomes:

$$\dot{S}'''_{\mathrm{gen}} = \frac{1}{T}\left(\frac{\partial q_x}{\partial x} + \frac{\partial q_y}{\partial y}\right) - \frac{1}{T^2}\left(q_x\frac{\partial T}{\partial x} + q_y\frac{\partial T}{\partial y}\right) + \rho c_p\frac{1}{T}\frac{\partial T}{\partial \tau} \tag{2}$$

Fourier law for an isotropic medium:

$$q_x = -k\frac{\partial T}{\partial x}\mathrm{d}y, \quad q_y = -k\frac{\partial T}{\partial y}\mathrm{d}x \tag{3}$$

where k is thermal conductivity.

Partial differential equation of heat conduction in 2-D co-ordinates:

$$\frac{\partial}{\partial x}\left(k\frac{\partial T}{\partial x}\right) + \frac{\partial}{\partial y}\left(k\frac{\partial T}{\partial y}\right) = \rho c_p\frac{\partial T}{\partial \tau} \tag{4}$$

Combining eq. (2) with eqs. (3) and (4), entropy generation rate is got:

$$\dot{S}'''_{\mathrm{gen}} = \frac{k}{T^2}\left[\left(\frac{\partial T}{\partial x}\right)^2 + \left(\frac{\partial T}{\partial y}\right)^2\right] \tag{5}$$

In fig. 1(a) (model 1), the thermal concentrator was made of 20 Cu wedges and 20 PDMS wedges which were set in stainless steel substrate [15]. The computational domain was a 240 × 200 mm plate, with the high constant temperature, T_H, and the low constant temperature, T_L. Initial temperature and T_L were set to 273 K. Thermal conductivities of Cu, PDMS, and stainless steel were k_{Cu} = 394, k_{PDMS} = 0.15, and k_b = 16, respectively. There were two contrast model: material of concentrator is Cu totally in fig. 1(b) (model 2) and a plate without concentrator in fig. 1(c) (model 3). Different operating conditions were considered to investigate effect of temperature difference, namely T_H = 333 K (ΔT = 60 K), T_H = 373K (ΔT = 100 K), and T_H = 413 K (ΔT = 140 K). For exploring the effect of unit distance, it was also to discusses different unit distances with d = 4 mm (model 4) and d = 8 mm (model 5) in fig. 1(d).

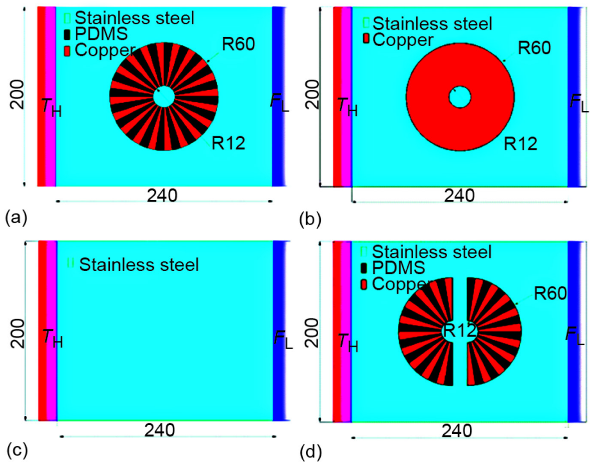

Figure 1. Computational model: (a) construction of thermal concentrator and computational domain (model 1), (b) model 2, (c) model 3, (d) heat concentrator model with different unit distances (model 4 and model 5)

The thermal concentration ratio, ε, based on entropy generation can be defined:

$$\varepsilon = \frac{\dfrac{T - T_0}{T_0}}{\dfrac{\int\limits_A \left| \dot{S}'''_{\text{gen}} - \dot{S}'''_{\text{gen},0} \right| \text{d}A}{\int\limits_A \dot{S}'''_{\text{gen},0} \text{d}A}} \tag{6}$$

where A is the computational domain and T – the temperature of the center point (0, 0), T_0 – the temperature of the center point (0, 0) of reference model 3, and $\dot{S}'''_{\text{gen},0}$ – the entropy generation rate of reference model 3.

The value of denominator reflected the level of thermal conductivity irreversibility with thermal concentrator. Larger value meant that the heat concentrator made larger influence and the function of camouflage and attracting heat was worse. The value of numerator meant the temperature rise. Thermal concentrator can increase temperature quickly and its attracting heat function was better with larger numerator value. Although the physical meaning of numerator and denominator were different, they were dimensionless parameters. In view of this, ε could be used to evaluate the function of thermal concentrator comprehensively to analyze the trend of heat conduction process. In addition, numerical calculation results were got by ANSYS FLUENT14.0. Mesh was generated by ICEM CFD14.0 with quadrilateral mesh. The numbers of elements are 188737 (model 1), 191794 (model 2), 39601 (model 3), 231158 (model 4), and 190972 (model 5), respectively.

Results and discussion

The temperature distribution of three simulation models was shown in fig. 2. The combination of PDMS-Cu presented special ability in assembling heat. Model 2 can make the center region stay in higher temperature, but it cannot attract heat purposefully. The thermal concentrator in model 1 can guide heat efficiently, so the temperature of center region rises quickly and purposefully. Each part of SYSTEM unit was a long and thin radial-shape, with large difference of the physical parameter of the adjacent pact, so circumferential heat transfer is small.

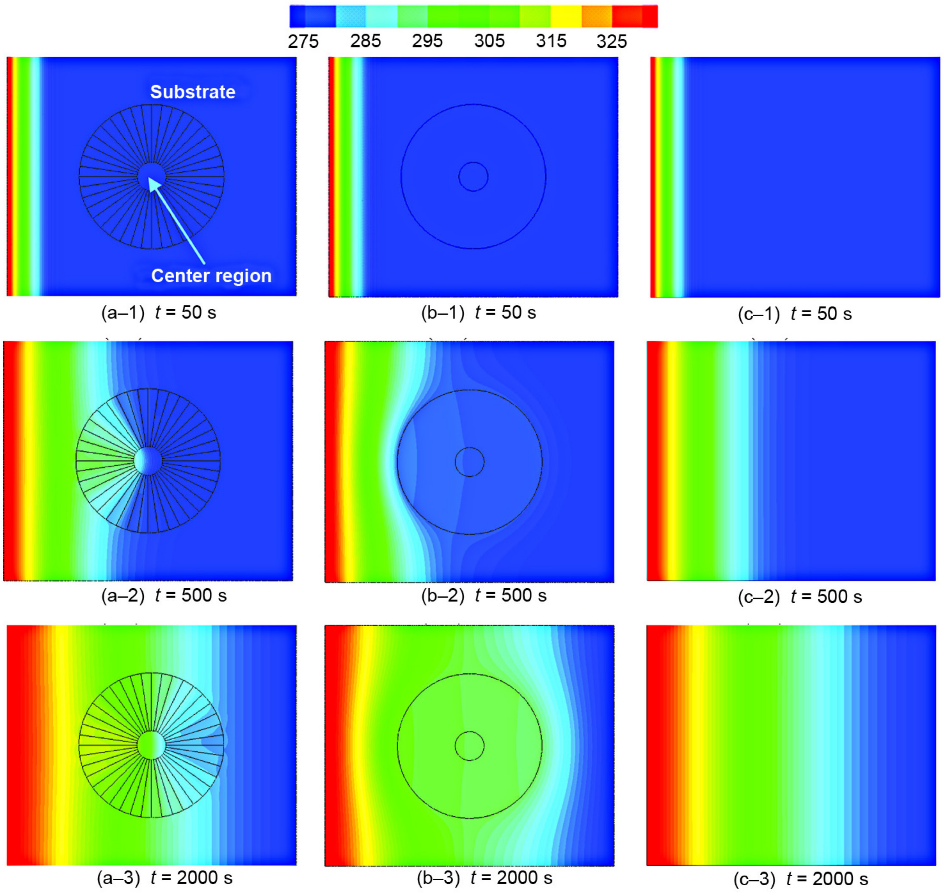

Figure 2. Temperature distribution of three simulation models: (a) model 1, (b) model 2, (c) model 3 *(for color image see journal web-site)*

The temperature distribution of the thermal concentrator seemed smooth, even the physical parameter of Cu and PDMS had large difference. Heat was imported to center region around 200 seconds, and it was balance dafter 2000 seconds in general. For the comparison of the two models, there is no distortion of isothermal line in model 1, *i. e.*, thermal concentrator had little effect on external environment, which reflected stealth characteristics.

To compare the heat transfer mechanism of different models, the distribution of entropy generation rate in different times was shown in fig. 3. When heat flux was near Cu ring, contours began to twist and grow with the progress of time. Near the junction of Cu ring and stainless steel substrate, dashed oval frame in fig. 3(b-2), entropy generation rate was in a higher level all the time. Compared to model 2, temperature gradient was large in the center region of model 1, so entropy generation rate was in a high level. At the same time, in the junction of concentrator and substrate, dotted oval frame in fig. 3(a-2), entropy generation rate also had larger value. Except for regions of the junction of center region and Cu sector of concentrator, solid oval frame in fig. 3(a-2), temperature distribution was smooth and entropy generation rate was small inside of thermal concentrator. Thermal concentrator can assure low dissipation in most areas. In addition, based on the contour of entropy generation rate, thermal concentrator also showed the function of heat stealth.

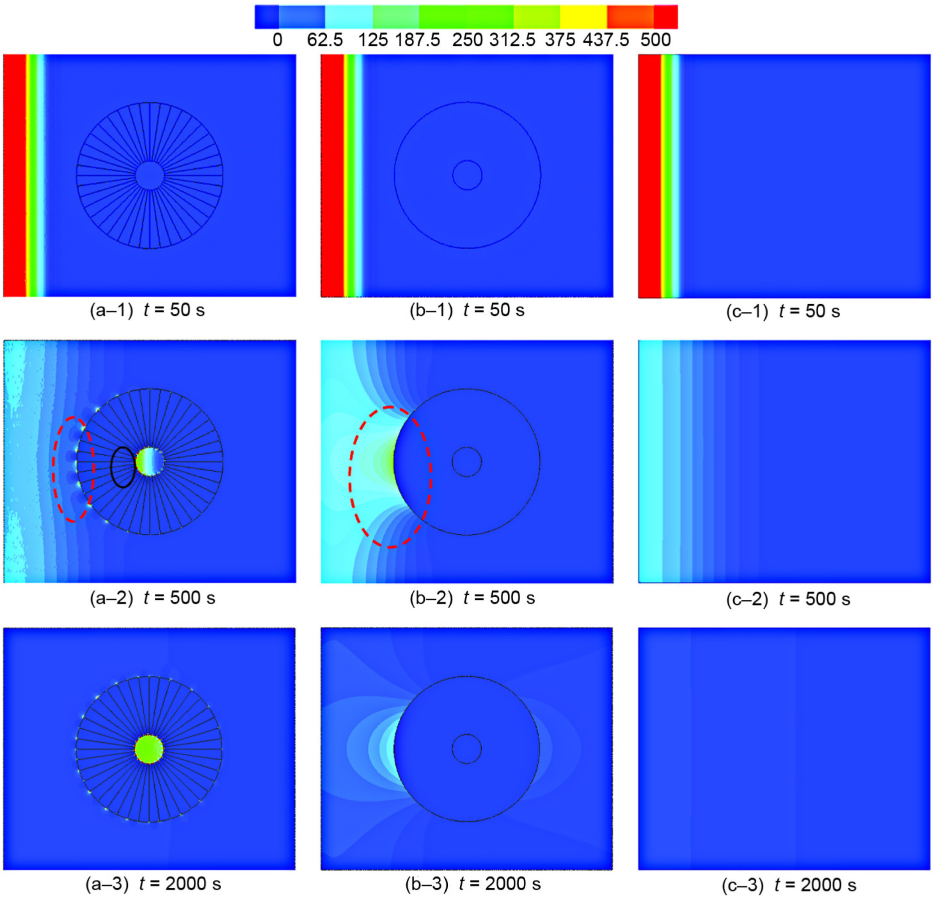

Figure 3. Entropy generation rate distribution of three simulation models: (a) model 1, (b) model 2, (c) model 3 *(for color image see journal web-site)*

Figures 4 and 5 showed the changing curve of temperature and entropy production rate on the three points with time, respectively. Figure 4(a) showed a quick temperature rise on the left side of concentrator interior, the value keeps a higher level all the time with the stable value of nearly 318 K. In addition, Cu model was the lowest and the stable value was only about 300 K. In this view, thermal concentrator can introduce heat within the structure rapidly. Model 2 showed that proximity of Cu ring and the center region had a similar temperature, so the temperature had the lowest level in fig. 4(a) and the highest level in fig. 4(c). The temperature rise rate of the center point was to represent the ability of attracting heat. Center point in model 1 with concentrator had the highest rise rate. Figure 4(c) showed that the cold side of the concentrator had lower temperature and the difference with plate model was nearly 5 K, and the concentrator also had good heat dissipation performance near a cold source.

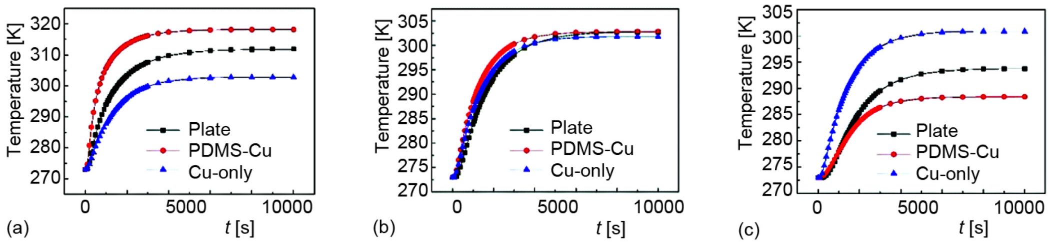

Figure 4. The temperature of three points: (a) A (-36, 0), (b) B (0, 0), (c) C (36, 0)

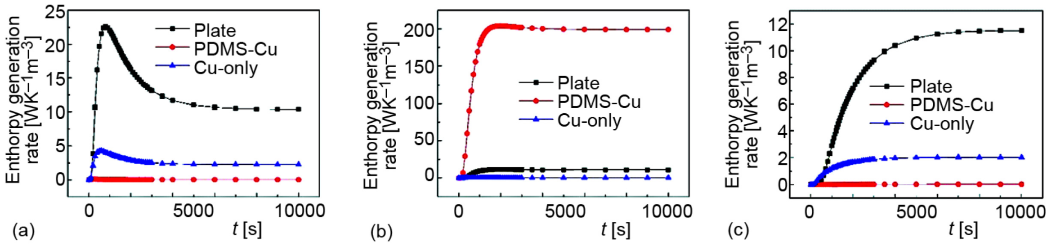

Figure 5. The entropy generation rate of three points: (a) A (-36, 0), (b) B (0, 0), (c) C (36, 0)

Entropy generation rate was gradually stable over time. At point A in plate model, entropy generation rate had an apace rise, and then decline. An extreme value appeared around 1000 seconds. In model 1, entropy generation rate of points A and C was almost near zero, and there was no irreversible loss inside. However, in the point B of the center region of substrate, entropy generation rate had an apace rise and a slight decline and then, it stayed in higher lever, nearly 200 W/Km^3 at last. There was large value of entropy generation rate in center region and most of the irreversible loss had concentrated in that region.

Differences between calculation model and contrast model by the integral on whole calculation domain were discussed based on entropy generation rate. Combining the rise of temperature of point B, ε was put forward to evaluate the thermal performance of the thermal concentrator. fig. 6(a) showed the comparison of ε in model 1 and model 2. In model 1, ε was at higher level. In initial time, the rise of entropy generation rate leaded to a sharp decrease of ε. A minimum appeared when heat was transferred to the cold side at around 1000 seconds. An extreme value appeared after a rise at around 3000 seconds and its value was about 0.2. Then heat conduction process tended to become stable and ε declined slightly to be stable. At the beginning, the thermal performance of thermal concentrator was best, and then it declined fast, with small rise.

From fig. 6(b), the trend of ε of time with different temperature difference was similar. The time of extreme points had no change with temperature difference. When ΔT = 140 K, ε had large value at initial time for large temperature rise at the center point. The difference of ε between ΔT = 60 K and ΔT = 100 K was similar to the difference between ΔT = 100 K and ΔT = 140 K. The increase of ε showed linear correlation with the increase of temperature

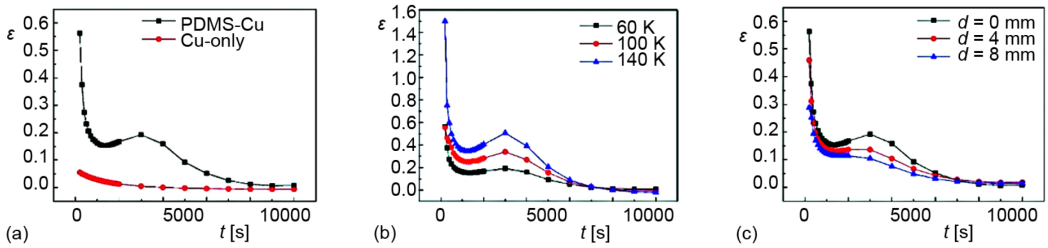

Figure 6. Heat concentration ratio: (a) ε of model 1 and model 2, (b) ε with different temperature difference, (c) ε with different center distances

difference. Figure 6(c) showed ε with different center distance. They showed similar trend with time and the time of extreme points had nuances. The smaller center distance, d, the greater ε was. When d = 8 mm (model 5), the change of ε became gentler and there was almost no maximum around 3000 seconds. At 3000 seconds, the values of ε different center distance were 0.2, 0.14, and 0.1, respectively. The initial increase of center distance had significant effect of ε. In addition, when d = 0 mm (model 1), ε had the biggest value.

Conclusions

In the current paper, a thermal concentrator was investigated through numerical simulation. According to aspects of temperature and entropy generation rate, thermal concentration ratio was defined and used for evaluating concentration effect. The thermal concentrator made of Cu wedges and PDMS wedges can achieve the function to control heat flux, which makes fast temperature rise at central region. Energy dissipation was low in most area of the concentrator, focusing on the center region and the junction of stainless steel and Cu sector of concentrator. Thermal concentration ratio of the concentrator was the largest at initial stage of heat conduction process. In addition, larger temperature difference or smaller center distance present better thermal control effect.

Acknowledgment

This work is supported by the Foundation for Innovative Research Groups of the National Natural Science Foundation of China (Grant No. 51421063) and the National Natural Science Foundation of China (Grant No. 51536001).

Nomenclature

A – computational domain, [–]
c_p – specific heat, [Jkg^{-1}K^{-1}]
d – unit distances, [mm]
k – thermal conductivity, [WK^{-1}m^{-1}]
q – heat flux, [Wm^{-2}]
$\dot{S}'''_{gen}$ – entropy generation rate, [WK^{-1}m^{-3}]
T – temperature, [K]
t – time, [s]
x, y – co-ordinate component, [m]

Greek symbols

ε – thermal concentration ratio, [–]
ρ – density, [kgm^{-3}]
τ – time, [s]

Subscripts

H – high
L – low

References

[1] Veselago, V. G., *et al.*, The Left Hand of Brightness: Past, Present and Future of Negative Index Materials, *Nature Materials*, *5* (2006), 10, pp. 759-762
[2] Schurig, D., *et al.*, Calculation of Material Properties and Ray Tracing in Transformation Media, *Optics Express*, *14* (2006), 21, pp. 9794-9804

[3] Leonhardt, U., *et al*., Broadband Invisibility by Non-Euclidean Cloaking, *Science*, *323* (2009), 5910, pp. 110-112
[4] Chen, H., *et al*., Electromagnetic Wave Interactions with a Meta-Material Cloak, *Applied Physics Letters*, *99* (2007), 6, 063903
[5] Yan, M., *et al*., Cylindrical Invisibility Cloak with Simplified Material Parameters is Inherently Visible, *Physics Review Letters*, *99* (2007), 23, 233901
[6] Chen, H., *et al*., Transformation Media for Linear Liquid Surface Waves, *Europhysics Letter*, *85* (2009), 2, 24004
[7] Shen, X. Y., *et al*., Research Progress in Thermal Meta-Materials, *Physics*, *42* (2013), 3, pp. 170-180
[8] Fan, C. Z., *et al*., Shaped Graded Materials with an Apparent Negative Thermal Conductivity, *Applied Physics Letters*, *92* (2008), 25, 251907
[9] Brun, M., *et al*., Achieving Control of In-Plane Elastic Waves, *Applied Physics Letters*, *94* (2009), 6, 061903
[10] Li, J. Y., *et al*., A Bifunctional Cloak Using Transformation Media, *Journal of Applied Physics*, *108* (2010), 7, 074504
[11] Guenneau, S., *et al*., Transformation Thermodynamics: Cloaking and Concentrating Heat Flux, *Optics Express*, *20* (2012), 7, pp. 8207-8218
[12] Schittny, R., *et al*., Experiments on Transformation Thermodynamics: Molding the Flow of Feat, *Physics Review Letters*, *110* (2013), 19, 195901
[13] Han, T., *et al*., Experimental Demonstration of a Bilayer Thermal Cloak, *Physics Review Letters*, *112* (2014), 5, 054302
[14] Lan, C., *et al*., Independent Manipulation of Electric and Thermal Fields with Bilayer Structure, *arXiv preprint arXiv*:1502.01325, Cornell University, Ithaca, N. Y., USA, 2015
[15] Han, T., *et al*., Manipulating Steady Heat Conduction by Sensu-Shaped Thermal Meta-materials, *Science Reports*, *5* (2015), May, 10242
[16] Nguyen, D. M., *et al*., Active Thermal Cloak, *Applied Physics Letters*, *107* (2015), 12, 121901
[17] Gyftopoulos, E. P., On the Evolution of the Definition of Entropy from Clausius to Today, *Journal of Energy Resources Technology*, *137* (2015), 2, 021010
[18] Bejan, A., *Entropy Generation through Heat and Fluid Flow*, John Wiley & Sons, New York, USA, 1982

Paper submitted: December 4, 2015
Paper revised: February 22, 2016
Paper accepted: March 9, 2016